

# High Accuracy Split Ring Resonator Based Sensor with Polynomial-Assisted Dielectric Characterization for Solid Material

Mohammad Harris Misran, Maizatul Alice Meor Said, Mohd Azlishah Othman, Samsul Setumin, Norazian Subari, Suleiman Aliyu Babale, *Member, IEEE*

**Abstract**—These days, the characterization of material permittivity has gained significant interest from researchers. Even though conventional measurement techniques able to provide high accuracy of measurement, many of the devices still suffer from bulky size, expensive fabrication and complex design structures. To overcome these issues, a compact split ring resonator (SRR) based sensor was proposed for high accuracy material characterization. The proposed sensor operates at a stable resonant frequency of 3.854 GHz and utilizes multiple offset resonant frequencies combined with polynomial fitting analysis to improve dielectric constant extraction accuracy. Experimental validation using Rogers 5880, Rogers 4350, and FR4 substrates demonstrates dielectric constant accuracies of 98.67%, 88.36%, and 97.14%, respectively, while loss tangent accuracy exceeds 99% for all tested materials. The optimized 12mm x 12mm sensor on FR4 also provides stable resonance response, low loss and high Q-factor, making it suitable for low-cost and reliable microwave sensing applications.

**Index Terms**— Dielectric Constant, High Accuracy Sensor, Material characterization, Split Ring Resonator (SRR)

## I. INTRODUCTION

In recent years, microstrip antenna technology has advanced rapidly due to its widely used in modern wireless and microwave communication systems. These antennas are commonly applied in satellite communications, radar systems, remote sensing, and portable wireless devices because of their compact design, lightweight structure, low cost and ease to integrate with planar circuits [1], [2]. Such characteristics make microstrip antennas highly attractive for compact and high-

performance applications in next-generation communication technologies [3], [4].

At the same time, the accurate characterization of electromagnetic material properties, particularly complex permittivity, has become increasingly important. The dielectric constant of a material strongly affects electromagnetic wave propagation, impedance matching, and the resonant behaviour of microwave components [5], [6]. As a result, precise permittivity measurement is required to improve the performance of antennas, filters and microwave sensors [7], [8]. At higher frequencies, where small variations in dielectric properties can significantly influence overall system performance, this requirement becomes even greater to ensure the accuracy of the measurement [9], [10].

The demand for reliable and low-cost material characterization techniques has increased because of the continuous growth of wireless communication technologies. With Accurate sensing methods are needed not only for device optimization but also for material verification and quality control in industrial applications due to the advancement of high speed communication systems and microwave-based devices. [11], [12].

Resonant cavity and transmission line methods, traditional permittivity measurement techniques, able to provide high accuracy measurement. However, these techniques limited by large design structures, complicated calibration process and high fabrication cost [13], [14]. In addition, they have low compatibility with planar techniques and caused the integration process into compact microwave systems become more challenging. Although planar microwave sensors have been introduced as an alternative solution, many existing designs still face compromises between sensitivity, accuracy, and structural simplicity [15], [16].

**Mohammad Harris Misran**, main author, is with Centre for Telecommunication Research & Innovation (CeTRI), Fakulti Teknologi dan Kejuruteraan Elektronik dan Komputer (FTKEK), Universiti Teknikal Malaysia Melaka (UTeM), Hang Tuah Jaya, 76100, Durian Tunggal, Melaka, Malaysia (email: harris@utem.edu.my)

**Maizatul Alice Meor Said** is with Centre for Telecommunication Research & Innovation (CeTRI), Fakulti Teknologi dan Kejuruteraan Elektronik dan Komputer (FTKEK), Universiti Teknikal Malaysia Melaka (UTeM), Hang Tuah Jaya, 76100, Durian Tunggal, Melaka, Malaysia (email: maizatul@utem.edu.my)

**Mohd Azlishah Othman** is with Centre for Telecommunication Research & Innovation (CeTRI), Fakulti Teknologi dan Kejuruteraan

Elektronik dan Komputer (FTKEK), Universiti Teknikal Malaysia Melaka (UTeM), Hang Tuah Jaya, 76100, Durian Tunggal, Melaka, Malaysia (email: azlishah@utem.edu.my)

**Samsul Setumin** is with Centre for Electrical Engineering Studies, Universiti Teknologi MARA Cawangan Pulau Pinang, Permatang Pau, Malaysia (email: samsuls@uitm.edu.my)

**Norazian Subari** is with Faculty of Electrical and Electronics Engineering Technology, Universiti Malaysia Pahang Al-Sultan Abdullah, Malaysia (email: aziansubari@umpsa.edu.my)

**Suleiman Aliyu Babale** is with Department of Electronics and Telecommunications Engineering, Ahmadu Bello University, Zaria, Nigeria (email: sababale@abu.edu.ng)

Recently, resonator-based sensing methods have attracted significant attention, especially those based on metamaterial-inspired structures such as SRRs. SRRs are well known for their strong electromagnetic field confinement and high sensitivity to dielectric variations, making them suitable for material characterization applications [17], [18]. Different SRR configurations, including complementary SRRs and multi-mode resonators, have been investigated to improve sensing capability and measurement performance [19], [20]. Despite these developments, several limitations remain.

Many reported SRR based sensors depend mainly on single-resonance frequency analysis, which can reduce the reliability and accuracy of dielectric extraction, particularly for materials with nonlinear or frequency-dependent characteristics [21], [22]. Furthermore, linear approximation relationships are often used to estimate dielectric properties from resonant frequency shifts, which may produce significant errors in real measurements. Some of the microwave sensor design also has complicated structures or involved multilayer design that increase fabrication complexity and entire cost [18], [23]. When several SRR shapes such as circular, square and hexagonal geometries have been compared in term of their performance, a comprehensive analysis of their sensing stability and sensitivity is still limited [24], [25].

In addition, SRR based sensors inherently suffer from several practical limitations. These structures generally exhibit relatively low quality factor (Q-factor) values, producing broader resonance responses that reduce frequency resolution and sensing precision [19], [20]. Their performance is also highly sensitive to fabrication tolerances, where small variations in gap size, conductor width, or etching accuracy can cause measurable shifts in resonant frequency. Compared to circular geometries, square SRR structures may also provide less uniform electromagnetic field confinement, reducing interaction efficiency with the material under test (MUT), especially for materials with low dielectric contrast [24], [25]. Moreover, relying solely on single-frequency analysis further limits the robustness of dielectric characterization. These issues highlight the need for improved sensor designs and more advanced analysis methods to enhance measurement reliability and accuracy.

To overcome these limitations, this paper presents a high accuracy SRR based microwave sensor that analyze the shifted resonant frequencies set using a polynomial fitting assisted technique for dielectric constant characterization. By utilizing 2<sup>nd</sup> and 3<sup>rd</sup> order polynomial analysis, the proposed sensor able to determine the nonlinear relationship between resonant frequency shifts and permittivity properties more effectively, leading to increase the accuracy of material characterization [21], [22]. In addition, a comparative study of different SRR geometries is performed to identify a configuration with better sensing stability and performance. The proposed sensor employs a compact planar structure with the SRR integrated into the ground plane, allowing simple fabrication and easy integration with standard microwave circuits.

## II. DESIGN AND METHOD

Different shapes of SRR were designed and simulated to obtain the most suitable resonator performance at desired frequency. Designing of split ring resonator by using different shapes (circular, square and hexagon) and different sizes create different resonant frequencies as shown in Fig. 1 and Fig. 2. Therefore, the resonant frequency of different shapes and sizes of split ring resonator can be used to determine the relationship between resonant frequency, sizes and shapes of split ring resonator.

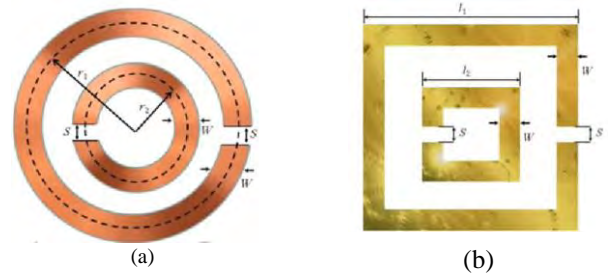


Fig. 1: (a) Circular SRR (C-SRR) (b) Square SRR (S-SRR)

$$\begin{aligned} \text{Average loop length,} \\ L_{1,2} &= 2\pi r^{1,2} - S \\ \text{Resonant frequency for} \\ \text{single loop, } f_{1,2} &= \\ \frac{c}{2L_{1,2}\sqrt{\epsilon_{eff}}} \end{aligned}$$

$$\begin{aligned} \text{Average loop length,} \\ L_{1,2} &= 4l_{1,2} - S - 4W \\ \text{Resonant frequency for} \\ \text{single loop, } f_{1,2} &= \\ \frac{c}{2L_{1,2}\sqrt{\epsilon_{eff}}} \end{aligned}$$

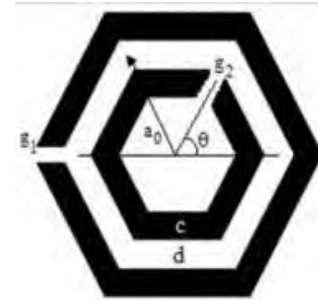


Fig. 2: Hexagon SRR (H-SRR)

Resonant frequency for single loop,

$$\begin{aligned} f_o &= \frac{1}{(2\pi\sqrt{(2a_{eq} \cdot L_{Net} \cdot C_{Net})})} \\ N &= 6, a_{eq} = 2a \left( \sin\left(\frac{\pi}{2}\right) \right) - \frac{g}{N} \\ L_{Net} &= 0.00508 \left( 2.030 \log_{10} \frac{4l}{c} - 2.636 \right) \\ C_{Net} &= \frac{(N \sin\left(\frac{\pi}{N}\right) + \beta)^2 - \left(\frac{\Delta}{a}\right)^2}{2(N \sin\left(\frac{\pi}{N}\right) + \beta)} \end{aligned}$$

Fig. 3 illustrates the equivalent circuit model of the proposed SRR structure, while the resonant frequency equations for the different SRR geometries are expressed as follows:

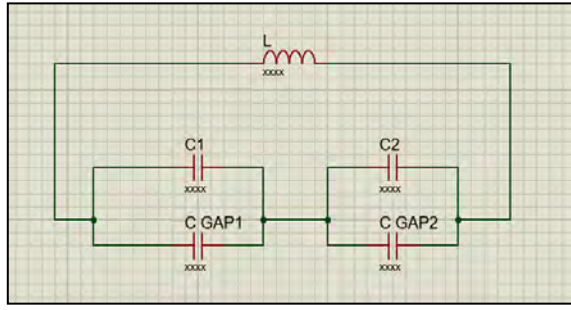


Fig. 3: Equivalent circuit of the SRR

For Circular - SRR :

$$f_0 = \frac{1}{2\pi\sqrt{LC_{eq}}} = \frac{1}{2\pi\sqrt{L_T \left[ \frac{(\pi r_0 - g)C_{pul}}{2} + \frac{\epsilon_0 ct}{2g} \right]}}$$

For Square - SRR :

$$f_0 = \frac{1}{2\pi\sqrt{L_T C_{eq}}} = \frac{1}{2\pi\sqrt{L_T \left[ \left(2a_{avg} - \frac{g}{2}\right) C_{pul} + \frac{\epsilon_0 ch}{2g} \right]}}$$

For Hexagon- SRR :

$$f_0 = \frac{1}{2\pi\sqrt{L_T C_{eq}}} = \frac{1}{2\pi\sqrt{L_T \left[ \frac{(3a_{avg} - g_1)C_{pul}}{2} + \frac{\epsilon_0 ch}{2g_1} \right]}}$$

Among them,  $L_T$  is the total inductance of split ring resonator, and  $C_{eq}$  is the equivalent capacitance of the structure, calculated according to the equivalent circuit.  $C_{pul}$  is the capacitance per unit length,  $r_0$  (C-SRR) and  $a_{avg}$  (S-SRR and H-SRR) between the rings are the distance from the center of the two components of the SRR.  $C_{pul}$  is calculated as

$$C_{pul} = \frac{\sqrt{\epsilon_e}}{c_0 Z_0}$$

where  $c_0 = 3 \times 10^8 \text{ m s}^{-1}$  is speed of light.  $\epsilon_e$  is the effective permittivity of the substrate and  $Z_0$  is the total impedance. The total inductance of the structures,  $L_T$  is computed as

$$L_T = 0.00508l \left( 2.303 \log_{10} \frac{4l}{d} - \theta \right)$$

where,  $l$  and  $d$  are the wire length and width, respectively. The constant  $\theta$  varies with wire geometry and is given as 2.45 (Circular SRR), 2.85 (Square SRR) and 2.64 (Hexagonal SRR).

### III. RESULTS AND DISCUSSIONS

The resonant characteristics of S-SRR, C-SRR and H-SRR with different radius and metallic strip width,  $c$ , are investigated through analytical computation and full-wave simulation. The resonant frequencies of the proposed SRR structures are initially estimated using theoretical equations and subsequently verified through simulation results to evaluate the accuracy and behaviour of each geometry under dimensional variations. Different SRR shapes produce sharp resonant characteristics because current distribution and electromagnetic field confinement is altered and optimized within the resonator structure.

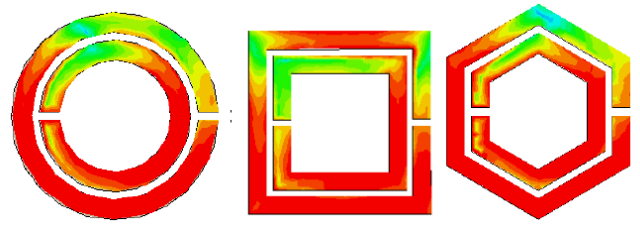


Fig. 4 C-SRR, S-SRR, H-SRR

Fig. 4 present investigation of the surface current distributions analysis for different SRR structures. In current distribution analysis, red colour and green colour represent the highest current density and the lowest current density, respectively. From the observation, it shows that each SRR geometry has different current concentration patterns, particularly between the split gap and ring edges. These differences give significant impact to the resonant behaviour, quality factor, and electromagnetic coupling capability of the resonator. The surface current distributions in the circular and hexagonal structures are smoother and have more uniform current flow compared to the square SRR. S-SRR has stronger field concentration at the sharp corners compare to other area. Therefore, detailed analysis of the SRR geometry and current distribution is required to optimize the SRR performance and improve the overall effectiveness of the proposed sensor design.

COMPARISON OF DIFFERENT SIZE FOR VARIOUS SHAPES

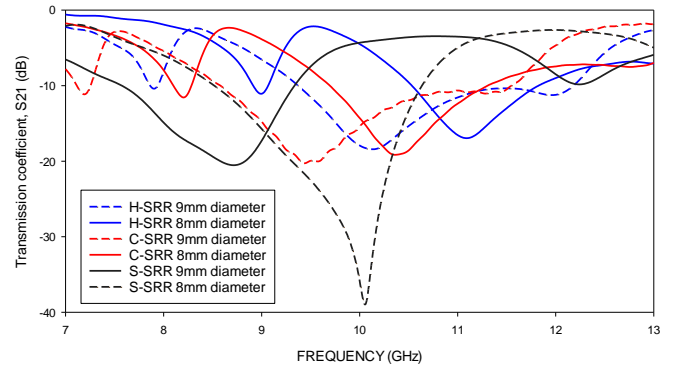


Fig. 5: Comparison of S-parameters between different shapes, ring widths, and diameters of SRRs

Fig. 5 shows the performance comparison of the designed sensor with different SRR geometries and SRR sizes. Based on the simulated results, both the H-SRR and C-SRR demonstrate better stability in resonant frequency characteristics when the SRR size is varied. In contrast, the square SRR exhibits larger resonance deviations under the same dimensional variations, indicating higher sensitivity to geometrical changes. The improved stability observed in the H-SRR and C-SRR structures can be attributed to their more uniform current distribution and smoother electromagnetic field confinement, which contribute to consistent resonant behaviour.

COMPARISON OF GAP FOR VARIOUS SHAPES

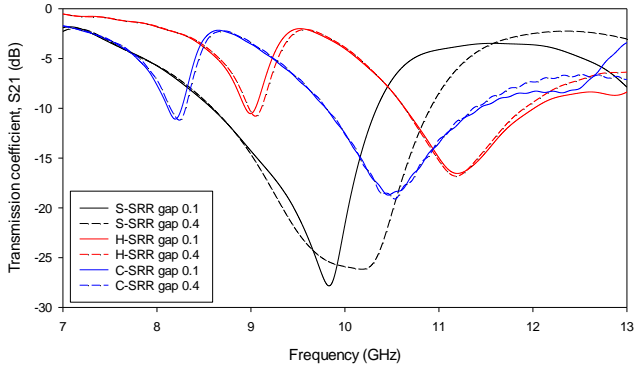


Fig. 6: Comparison of S-parameters between different shapes and split gap dimension of SRR

The performance comparison for different split gap in the SRR structure is presented in Fig. 6. From the observation, the H-SRR and C-SRR has similar trends and maintain stable resonant responses compared to the S-SRR as the gap size varies. The S-SRR shows more significant resonance shifting and performance fluctuation due to the stronger field concentration at the sharp edges and corners. In addition, the C-SRR produces a deeper resonance characteristic than the H-SRR, showing stronger electromagnetic coupling and higher resonance quality. A deeper resonance is required as it enhances the sensitivity and detection capability of the sensor.

SENSOR PERFORMANCE WITH VARIOUS GAP SIZE

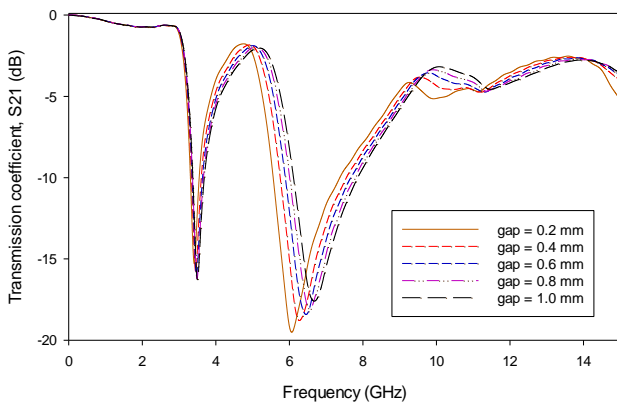


Fig. 7: Resonant frequency of different gap size

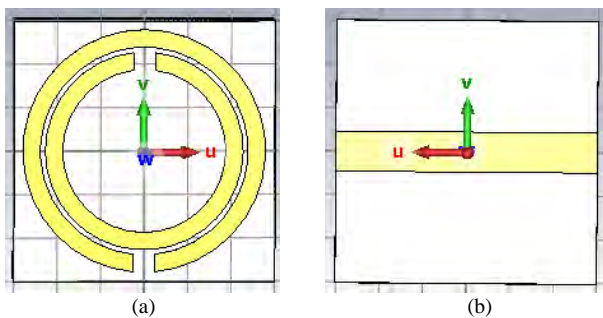


Fig. 8 (a) Top View and (b) Bottom View

Fig. 7 shows the transmission coefficient response of the proposed SRR sensor for different gap sizes. The resonant frequency at 3.854 GHz demonstrates greater stability against

gap variation compared to the resonance near 6 GHz, which exhibits larger frequency shifts. This indicates that the lower-frequency resonance is less sensitive to fabrication tolerance and dimensional deviation. The SRR size was optimized and reduced to 5.6 mm to achieve resonance at 3.854 GHz while maintaining compactness as shown in Fig. 8. Lower-frequency operation offers several advantages, including reduced conductor and dielectric losses, lower noise sensitivity, improved resonance stability, and more reliable dielectric characterization performance for microwave sensing applications.

After the optimization completed, the proposed sensor was simulated using multiple MUTs with different dielectric constant values to investigate the resonant response behaviour. Different resonance frequencies were generated for each MUT because each MUT has a unique permittivity value. The produced resonance shifts were carefully observed and analyzed. The relationship between the shifted resonance frequency and the dielectric constant of the MUTs is extracted and generated. The results demonstrated a clear resonance frequency shift for each material, confirming the high sensitivity of the proposed sensor with different dielectric constant.

RESONANT FREQUENCY OF DIFFERENT DIELECTRIC CONSTANT

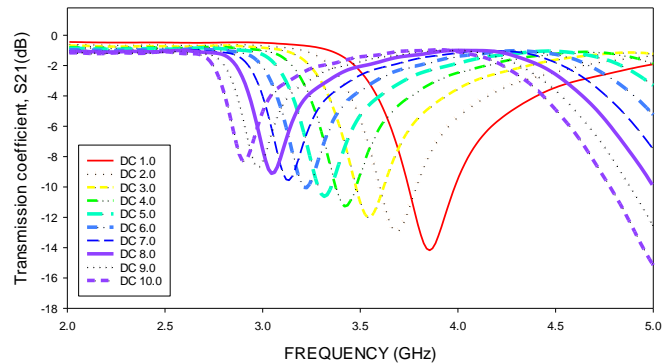


Fig. 9: Resonant frequency of different dielectric constant

DIELECTRIC CONSTANT VS SHIFTED FREQUENCY

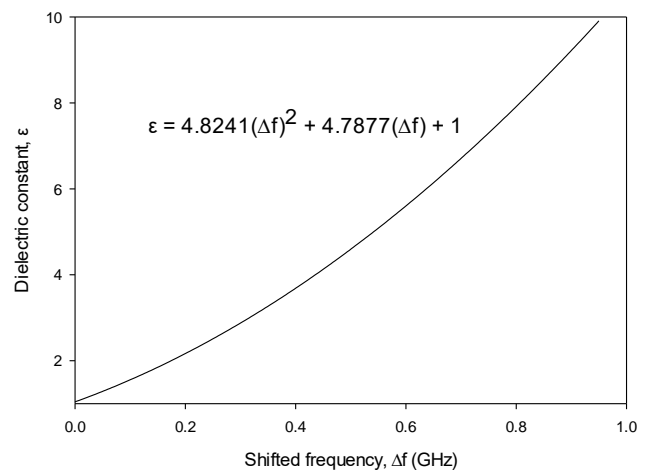


Fig. 10: Shifted frequency of different dielectric constant

Fig. 9 and Fig. 10 shows the resonance frequency shifting response respected to the initial resonance frequency against the

dielectric constant of MUT in polynomial equation form. These graphical representations provide significant insight into the dielectric characteristic of the MUTs and their impact on the resonant properties of the resonator.

TRANSMISSION COEFFICIENT OF DIFFERENT MUT

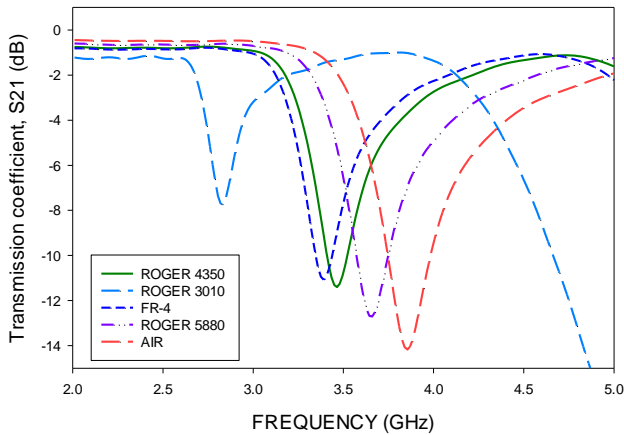


Fig. 11: Resonant frequency of different material under test (MUT)

LOSS TANGENT VS SHIFTED FREQUENCY

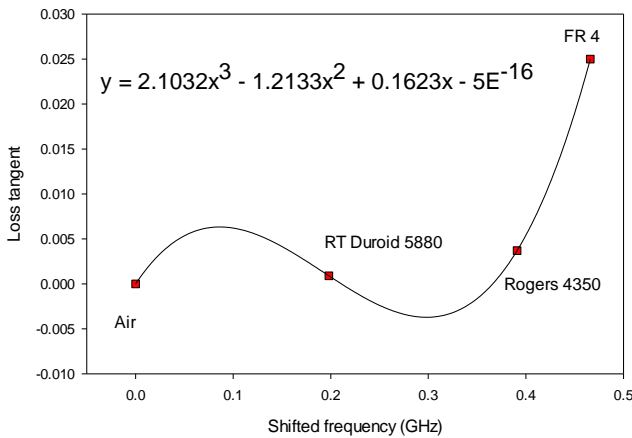


Fig. 12: Shifted frequency of different loss tangents

In Fig. 11, different MUT, such as Roger 5880, Roger 4350, Roger 3010, and FR4, were analyzed. The shift in resonant frequency for each MUT is being examined and studied. The observation shows that each MUT produces significant impacts on the resonant frequency. This variation is taken for further consideration and analysis to accurately characterize the dielectric constant of each material. Such characterization is essential for optimizing the application of these materials in high frequency electronic circuits and improving their performance in real engineering scenarios.

Fig. 12 shows the polynomial curve of the loss tangent against the shifted frequency for different MUT. To further characterize the relationship between resonance response and dielectric properties, 2<sup>nd</sup> order and 3<sup>rd</sup> order polynomial equations were extracted from the plotted graph using equation (1) and equation (2) to estimate the dielectric constant and loss tangent of the measured MUTs, respectively. The exact polynomial equations are presented together with the plotted graphs as reference equations for the proposed sensor design.

$$y = Ax^2 + Bx + C \quad (1)$$

$$y = Ax^3 + Bx^2 + Cx + D \quad (2)$$

The C-SRR then fabricated successfully on FR4 substrate and measured to verify the simulation result. Fig. 13 shows the fabricated C-SRR microwave sensor from top and bottom view.



Fig. 13: (a) Front View and (b) Back View

Fig. 14 presents the comparison between the simulated and measured resonance responses for different MUTs. The simulation and measurement trendlines show strong agreement for all investigated MUTs, demonstrating that the developed microwave sensor is reliable and capable of accurately predicting the resonant behaviour of the proposed sensor. The high similarity between simulation and measurement also validates the effectiveness of the fabricated prototype under practical measurement situation.

SIMULATION VS MEASUREMENT OF VARIOUS MUT

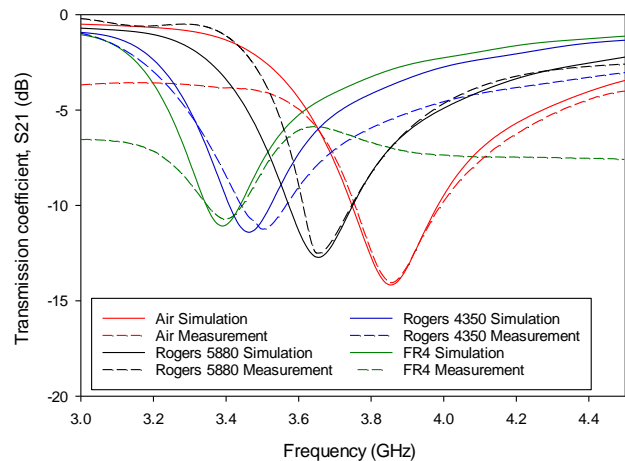


Fig. 14: Comparison between measurement and simulation of various MUT

TABLE I  
COMPARISON OF MEASUREMENT AND SIMULATION VALUE

	Air	Rogers 5880	Rogers 4350	FR4
<b>Simulation (GHz)</b>	3.854	3.656	3.463	3.388
<b>Measurement (GHz)</b>	3.858	3.651	3.508	3.399
<b>Error (%)</b>	<b>0.104%</b>	<b>0.137%</b>	<b>1.299%</b>	<b>0.325%</b>

Table I summarizes the comparison recorded data between the simulated and measured resonant frequencies for the different MUTs. Based on the results, the measured resonant frequencies show strong agreement with the simulated values, demonstrating the reliability and accuracy of the fabricated sensor design and simulation sensor. From the data, resonance frequencies is confirming decrease as the dielectric constant of the MUT increases, which is consistent with the theoretical

behaviour of microwave resonator sensors where higher permittivity materials increase the effective capacitance and resonance shifting toward lower frequencies.

The percentage error between simulation and measurement remains relatively small for all tested materials, ranging from 0.104% to 1.299%. The lowest error is contributed by air, while the highest deviation observed from Rogers 4350. Nevertheless, the overall inconsistency is still within an acceptable range for microwave sensing applications. These minor differences may be contributed by fabrication error, soldering impact, variation in substrate properties and environmental conditions during experimental validation. Overall, the results confirm that the proposed sensor achieves good measurement accuracy and stable resonant performance for dielectric characterization applications.

These insignificant errors can be attributed to a range of sources, including production flaws, the effects of soldering, and intrinsic losses in measuring equipment. These inaccuracies highlight the difficulties in establishing perfect consistency between theoretical simulations and experimental results. However, the high similarity between simulation and measurement results confirms the proposed simulation design and its predictive ability. This thorough comparison is essential for optimizing simulation models and increasing the correctness of future experimental designs in sensors.

SHIFTED RESONANT FREQUENCY VS DIELECTRIC CONSTANT

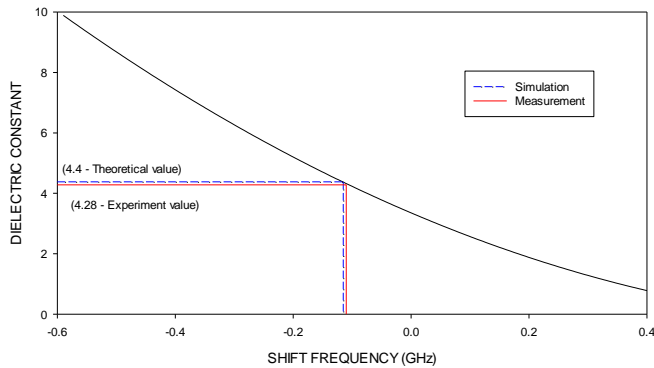


Fig. 15: Dielectric constant of FR4

Fig. 15 shows the graphical relationship between the dielectric constant and shifted resonance frequency of the investigated MUTs. Based on the plotted graph, the shifted frequency increases consistently as the dielectric constant increases, indicating that the proposed sensor is highly responsive to permittivity variations. The graph also demonstrates a stable and predictable trendline, which confirms the effectiveness of the proposed sensor for dielectric characterization and material identification applications.

Using the 2<sup>nd</sup> order and 3<sup>rd</sup> order polynomial equations extracted from the plotted graph, the dielectric constant and loss tangent values of each MUT were calculated and recorded accurately. The extracted values show good agreement with the reference dielectric properties, indicating that the proposed polynomial fitting method provides reliable prediction accuracy for material characterization. Minor deviations may be caused by fabrication tolerance and measurement uncertainty during the experimental process.

TABLE II  
SENSOR PERFORMANCE FOR VARIOUS MUT

	Air	Rogers 5880	Rogers 4350	FR4	
<b>Simulation (GHz)</b>	3.854	3.656	3.463	3.388	
<b>Measurement (GHz)</b>	3.858	3.651	3.508	3.399	
<b>Shifted Freq (GHz)</b>	0.004	0.203	0.346	0.455	
<b>Dielectric Constant</b>	<b>Reference</b>	1	2.2	3.66	4.3
	<b>Measured</b>	1.02	2.17	3.23	4.18
<b>Accuracy (%)</b>	98.08	98.67	88.36	97.14	
<b>Loss Tangent</b>	<b>Reference</b>	0	0.0009	0.02	0.022
	<b>Measured</b>	6.00E-16	0.000899	0.0199	0.02199
<b>Accuracy (%)</b>	100.00	99.89	99.50	99.95	
<b>BW (MHz)</b>	180	195	180	195	
<b>Q-Factor</b>	42.83	37.62	38.50	34.85	
<b>Sensitivity (MHz/εr)</b>	na	169.2	130.1	137.9	

Table II shows the performance validation of the proposed microwave sensor through comparison between simulated and measured values for various MUTs, namely air, Rogers 5880, Rogers 4350, and FR4. The measured resonant frequencies highly similar with the simulated results, indicating good agreement between simulation and experimental validation. The resonance frequency gradually shifts toward lower frequencies as the dielectric constant increases, confirming the sensor's capability in characterizing materials with different dielectric properties. The highest shifted frequency is observed for FR4 with 0.455 GHz, followed by Rogers 4350 and Rogers 5880, while air shows only a minimal shift of 0.004 GHz due to its low permittivity.

The proposed sensor able to determine the dielectric constant with high accuracy and validate the reliability of the proposed sensor. High dielectric constant accuracy values achieved for air, Rogers 5880, FR4 and Rogers 4350 are 98.08%, 98.67%, 97.14% and 88.36%, respectively. This fluctuation may be caused by fabrication tolerance, substrate inconsistency, or measurement uncertainty. Similarly, the extracted loss tangent values demonstrate excellent agreement with reference values, achieving accuracies above 99% for all MUTs.

Proposed microwave resonator provides bandwidth ranges between 180 MHz and 195 MHz and the Q-factor varies from 34.85 to 42.83. Air as MUT produces the highest Q-factor due to lower dielectric losses. Compared to FR4, the determined Q-factor is the lowest because of its higher loss characteristic. The sensitivity of the proposed sensor also good, with the highest sensitivity obtained for Rogers 5880 at 169.2 MHz/εr, followed by FR4 and Rogers 4350. Overall, the results confirm that the proposed sensor provides stable resonant characteristics, high accuracy, and good sensitivity for dielectric characterization applications.

#### IV. CONCLUSION

In conclusion, the proposed SRR based microwave sensor successfully characterized the dielectric properties of different materials with high accuracy and stable performance. The sensor demonstrated strong agreement between simulation and measurement results for Air, Rogers 5880, Rogers 4350, and FR4 substrates. The measured dielectric constant achieved

accuracy of 98.67% for Rogers 5880, 88.36% for Rogers 4350, and 97.14% for FR4, while the loss tangent measurement exceeded 99% accuracy for all tested materials. The optimized SRR structure provided stable resonance characteristics, good sensitivity, compact size, and improved tolerance against fabrication variation. In addition, the use of polynomial fitting analysis improved the reliability of dielectric characterization compared to conventional single-frequency methods. Overall, the proposed sensor offers a low-cost, compact, and easy-to-fabricate solution for high-accuracy microwave material characterization and sensing applications.

#### AUTHOR CONTRIBUTIONS

Misran conceptualized the research work, conducted the overall investigation, supervised the project development, and prepared the manuscript draft as the main corresponding author. Meor Said and Othman contributed to the development of the methodology framework, experimental design, and technical validation of the proposed system. Subari and Babale were responsible for data processing, analysis, interpretation of experimental results, and performance evaluation. Setumin contributed to the review and refinement of the manuscript, particularly in data interpretation and technical presentation. All authors reviewed and approved the final version of the manuscript.

#### ACKNOWLEDGMENT

The authors would like to acknowledge the Centre for Research and Innovation Management (CRIM), Fakulti Teknologi dan Kejuruteraan Elektronik dan Komputer (FTKEK) and Universiti Teknikal Malaysia Melaka (UTeM) for supporting this project.

#### REFERENCES

- [1] M. H. Misran et al., "Miniaturization of High Sensitivity Defected Ground Structure Based Microwave Sensor for Material Characterization," *Jurnal Kejuruteraan*, vol. 38 (1), pp. 289-300, 2026.
- [2] A. M. Siddiky, M. T. Islam, and M. Samsuzzaman, "A multi-split based square split ring resonator for multiband satellite applications with high effective medium ratio," *Results in Physics*, vol. 22, p. 103865, 2021.
- [3] S. Khanal, J. Fulton, and S. Shearer, "Remote sensing in agriculture: accomplishments, limitations, and opportunities," *Remote Sensing*, vol. 12, no. 22, p. 3783, 2020.
- [4] Z. Zhou, Y. Wang, and H. Zhao, "Coding DGS resonator sensor for ultrahigh Q-factor dielectric thickness detection," *Journal of Electromagnetic Waves and Applications*, vol. 35, no. 11, pp. 1464-1476, 2021.
- [5] R. A. Alahnomi, Z. Zakaria, E. Ruslan, A. A. M. Bahar, and M. A. M. Isa, "Review of recent microwave planar resonator-based sensors: Techniques of complex permittivity extraction, applications, open challenges and future research directions," *Sensors*, vol. 21, no. 7, p. 2267, 2021.
- [6] H. S. Roslan, M. A. M. Said, Z. Zakaria, and M. H. Misran, "Recent development of planar microwave sensor for material characterization of solid, liquid, and powder: a review," *Bulletin of Electrical Engineering and Informatics*, vol. 11, no. 4, pp. 2190-2203, 2022.
- [7] K. J. Dehning et al., "Split-ring resonator based sensor for the detection of amino acids in liquids," *Sensors*, vol. 23, no. 2, p. 645, 2023.
- [8] K. S. L. Parvathi and S. R. Gupta, "Ultrahigh-sensitivity and compact EBG-based microwave sensor for liquid characterization," *IEEE Sensors Letters*, vol. 6, no. 4, pp. 1-4, 2022.
- [9] T. Haq and S. Koziel, "Novel complementary multiple concentric split ring resonator for reliable characterization of dielectric substrates with

- high sensitivity," *IEEE Sensors Journal*, vol. 24, no. 10, pp. 16233-16241, 2024.
- [10] Y. J. Zhang et al., "A resonator-type sensor with enhanced sensitivity for noninvasively detecting the variation of permittivity of liquids," *IEEE Access*, vol. 10, pp. 76544-76553, 2022.
- [11] M. H. Misran et al., "High Accuracy Dual Split Ring Resonator - Defected Ground Structure based Microwave Sensor for Material Characterization," *Majlesi Journal of Electrical Engineering*, vol. 19, no. 3, p. 1-10, 2025.
- [12] H. Gan, W. Zhao, Q. Liu, and W. Yin, "Differential microwave microfluidic sensor based on microstrip complementary split-ring resonator structure," *Sensors*, vol. 21, no. 3, p. 891, 2021.
- [13] Z. Wei et al., "A high-sensitivity microfluidic sensor based on a substrate integrated waveguide re-entrant cavity for complex permittivity measurement of liquids," *Sensors*, vol. 18, no. 11, p. 4005, 2018.
- [14] L. Wang, "Microwave sensors for breast cancer detection," *Sensors*, vol. 18, no. 2, p. 655, 2018.
- [15] C. Teng et al., "An angular displacement microwave sensor with 360° dynamic range using multi-mode resonator," *IEEE Sensors Journal*, vol. 21, no. 3, pp. 2899-2907, 2021.
- [16] M. Martinic, T. Markovic, A. Baric, and B. Nauwelaers, "A 4 × 4 array of complementary split-ring resonators for label-free dielectric spectroscopy," *Chemosensors*, vol. 9, no. 12, p. 348, 2021.
- [17] K. Masrakin et al., "Microstrip sensor based on ring resonator coupled with double square split ring resonator for solid material permittivity characterization," *Micromachines*, vol. 14, no. 4, p. 790, 2023.
- [18] A. M. Siddiky et al., "Double H-shaped complementary split ring resonator with different orientations for quad-band satellite applications," *Results in Physics*, vol. 19, p. 103427, 2020.
- [19] M. H. Misran, M. A. M. Said, M. A. Othman, A. Salleh, S. Suhaimi and M. Z. Idris, "High Sensitivity Double Split Ring Resonator - Defected Ground Structure (DSRR-DGS) Based Microwave Sensors for Material Characterization," 2024 IEEE Asia-Pacific Conference on Applied Electromagnetics (APACE), pp. 440-443, 2024
- [20] Z. Sourkouhi, V. Balasubramanian, and M. H. Zarifi, "Optically modulated split ring resonator sensor for optical density analysis of liquid analytes in microwave regime," *IEEE Transactions on Microwave Theory and Techniques*, vol. 72, no. 2, pp. 1150-1159, 2024.
- [21] T. Haq, S. Koziel, and U. Ullah, "High-sensitivity complementary split ring resonator sensor for dielectric characterization," *IEEE Sensors Journal*, vol. 25, no. 2, pp. 2145-2154, 2025.
- [22] B. K. Tay, S. Kapoor, W. Yu, and S. Y. Huang, "High-Q non-invasive glucose sensor using microstrip line main field and split ring resonator," *IEEE Sensors Journal*, vol. 25, no. 1, pp. 1022-1031, 2025.
- [23] A. Javed et al., "A low-cost multiple complementary split-ring resonator based microwave sensor for dielectric characterization," *IEEE Access*, vol. 11, pp. 41235-41246, 2023.
- [24] J. F. Vallecchi, E. Shamonina, and C. J. Stevens, "Analytical model of the fundamental mode of 3D square split ring resonators," *Journal of Applied Physics*, vol. 125, no. 1, p. 014901, 2021.
- [25] H. Hanif, M. L. Hakim, and T. Alam, "Highly sensitive miniaturized labyrinth shape circular split ring resonator based microwave sensor for low permittivity characterization applications," *AEU - International Journal of Electronics and Communications*, vol. 177, p. 155216, 2024.



**Mohamad Harris Misran** received the B.Eng. degree in Electronics Engineering (Telecommunication) from University of Surrey in 2006, and the M.Eng. degree in Telecommunication Engineering from University of Wollongong in 2008. He obtained the Ph.D. degree in Electrical Engineering from Universiti Teknikal Malaysia.

He is currently a Senior Lecturer with Universiti Teknikal Malaysia Melaka, where he has been serving since 2006. His research interests include antenna design, microwave sensors, metamaterial structures, wireless power transfer, Internet of Things (IoT) applications, and RF/microwave engineering. His current research focuses on metamaterial-inspired microwave

sensing systems, ultra-wideband antennas, and wireless power transfer technologies for advanced communication and sensing applications.



**Maizatul Alice Meor Said** received the B.Eng. degree in Electronics Engineering (Telecommunication) from University of Surrey in 2006, and the M.Eng. degree in Telecommunication Engineering from University of Wollongong in 2009. She later obtained the Ph.D. degree from Universiti Teknikal Malaysia Melaka.

She is actively involved in research and academic activities in the field of RF and microwave engineering. Her research interests include RF energy harvesting systems, resonators, microwave amplifiers, antennas, and microwave sensors. Her current research focuses on the development of efficient RF and microwave technologies for wireless communication, sensing, and low-power energy harvesting applications. She has also been involved in various research projects related to antenna design, resonator optimization, and microwave sensing techniques for advanced engineering applications.



**Mohd Azlishah Othman** received the Bachelor of Engineering degree in Electrical Engineering (Telecommunication) from Universiti Teknologi Malaysia in 2003. He obtained the Master's degree in Computer and Communication Engineering from University of Nottingham in 2005, and later received his Ph.D. degree in Electrical and Electronic Engineering at the same university.

In 2005, he joined Universiti Teknikal Malaysia Melaka, where he currently serves as a Senior Lecturer. He has been actively involved in academic, research, and technology development activities related to RF and microwave engineering. His research interests include RF and microwave circuits, microwave devices, wireless communication systems, and technology management. In recent years, his research has expanded into artificial intelligence (AI) applications, particularly involving intelligent systems, data-driven engineering solutions, and AI integration in communication and electronic technologies. He has also contributed to multidisciplinary research projects involving advanced engineering innovation and emerging digital technologies.



**Samsul Setumin** received the B.Eng. Degree (Hons.) in Electronic Engineering from University of Surrey in 2006, and the M.Eng. degree in Electrical-Electronic and Telecommunication Engineering from Universiti Teknologi Malaysia in 2009. He obtained the Ph.D. degree in the imaging field from Universiti Sains Malaysia in

2019.

Since 2010, he has been serving as a Lecturer with Universiti Teknologi MARA. Prior to his academic career, he worked as

a Test Engineer with Agilent Technologies and Intel Malaysia for approximately one year, where he was involved in electronic testing and validation activities. His research interests include computer vision, image processing, pattern recognition, embedded system design, and intelligent imaging systems. His current research focuses on AI-assisted vision systems, automated image analysis, and embedded technologies for real-time engineering applications.



**Norazian Subari** is a lecturer at the Faculty of Electrical and Electronics Engineering Technology, Universiti Malaysia Pahang Al-Sultan Abdullah, UMPSA with 17 years of teaching experience since 2009. She previously gained industry experience at Malaysia Marine and Heavy Engineering, MMHE, Pasir Gudang, Johor. She holds a Bachelor of Science in Electrical Engineering from Universiti Teknologi MARA, UiTM, and a Master of Science in Electrical and Electronic Engineering (Sensors and Instrumentation) from Universiti Sains Malaysia, USM.

With nearly two decades of professional experience, including over a decade in academia, her research interests include sensors, artificial intelligence, signal processing, and engineering education. With a strong commitment to engineering education, she has guided student projects that were successfully designed, implemented, and demonstrated as functional systems, reflecting her emphasis on practical application and creative problem-solving. In recognition of her contributions, she was awarded the Anugerah Khas YB Menteri Pendidikan Tinggi: Rekabentuk Kurikulum dan Penyampaian Inovatif (AKRI) 2024 by the Ministry of Higher Education (KPT).



**Suleiman Aliyu Babale** (Member, IEEE) received his B.Eng. degree in Electrical Engineering from Bayero University, Kano, in 2005, and an M.Sc. in Electrical Engineering from Ahmadu Bello University, Zaria, in 2012. He earned his Ph.D. in Electrical Engineering, with a specialization in Telecommunications, from Universiti Teknologi Malaysia in 2018.

He is currently an Associate Professor in the Department of Electronics and Telecommunications Engineering at Ahmadu Bello University, Zaria. He has authored over 50 scholarly publications in areas such as Internet of Things (IoT), antenna design, and wireless communication systems for 5G, which have collectively attracted more than 400 citations on Google Scholar.

Dr Babale has successfully led and managed multiple research and development grants, contributing to advancements in wireless technologies and smart systems. Dr. Babale is a registered engineer with the Council for the Regulation of Engineering in Nigeria (COREN) since 2011 and is an active member of the Institute of Electrical and Electronics Engineers (IEEE).